International Journal of Modern Manufacturing Technologies
ISSN 2067–3604, Vol. XII, No. 2/2020

MODELING OF HEAT DISTRIBUTION AT THE SPINDLE BEARING TEST RIG

Mateusz Muszyński, Jan Kosmol, Andrzej Sokołowski

Silesian University of Technology, Faculty of Mechanical Engineering, Department of Machine Technology
Konarskiego 18A, 44-100 Gliwice, Poland

Corresponding author: Mateusz Muszyński, mateusz.muszynski@polsl.pl

Abstract: The paper presents a way of modelling the heat and temperature distribution on a test rig using the finite element method. An extended bearing contact model was adopted to model the magnitude of the contact forces which motion resistance and power of the heat source were determined from. The extended contact model of the bearing was used very rarely in previous considerations. The method of determination of convection coefficients, the calculations of which are based on the relationships presented in the literature, is also presented. Correct determination of heat source power and convection coefficients is a key issue in temperature field modelling. The paper contains sample results of model and experimental research for preload of a selected values and various bearing speeds. It has been proven that it is possible to correctly estimate the temperature filed using analytical calculations and FEM simulations.
Key words: angular bearing, contact model, heat loss, FEM.

1. INTRODUCTION

The heat emitted by a machine tool during operation plays an important role in terms of machining accuracy. There are plenty of sources of heat, such as hot chips, motors, bearings, etc. Particularly important units in terms of machining accuracy are electrospindles of machine tools, where the main sources of heat are the electric motor and bearings. Due to their closed form, electro-spindles require a dedicated cooling system. The heat generated during operation can significantly affect the axial or radial displacement of the spindle tip. As a result, the tool is subjected to displacements which are multiplied in the radial direction due to the tool length. Improving the accuracy of machine tools involves the capability of estimating the amount of heat generated in spindle bearings to optimize the form of the bodies or to be able to introduce displacement correction into machine controller.
Thermal phenomena modelling may significantly contribute to shortening the design time of an optimal body form, without the need to construct any prototypes. Such a situation will be the case when the applied theoretical models are verified by experimental research, therefore model research is closely linked to experimental research. The heat transfer and temperature field are most easily modelled using the finite element method (FEM). However, to correctly estimate the temperature field, e.g. of a machine body, it is necessary to adopt appropriate models of heat sources and heat exchange mechanisms.
Angular contact ball bearings are commonly used for bearing purposes in fast-running spindles of machine tools [19], which are characterized by plenty of advantages, such as relatively low motion resistance, ability to transfer longitudinal and transverse loads, simplicity of bearing assemblies and affordable price. Due to the complex kinematics of ball motion, modelling angular contact bearings is laborious and requires numerous calculations. The angular contact bearing heat loss model is the subject of numerous research activities and is constantly being developed.
The heat source model of a bearing requires the determination of its motion resistance moment, as the power in rotary motion is the product of torque and angular velocity. Nevertheless, determining the motion resistance moment is not an easy task, and it requires some prior calculations of reaction forces between the ball and the raceway under given conditions (preload, rotational speed or external loads). The magnitude of these reactions (contact forces) depends significantly on mentioned above factors, mainly speed and load. Contact forces, which can be determined analytically or using the finite element method, have been the subject of numerous research papers. However, it needs to be borne in mind that only a few works on contact forces modelling consider the possibility of radial expansion of a rotating ring. The limitation of radial expansion of this ring caused by the presence of balls was considered sporadically [9, 15].
Knowing the internal load condition of the bearing (the magnitude of the contact forces), it is possible to determine the motion resistance based on theoretical models. An extremely important issue when modelling the temperature field using FEM is to

assign appropriate values for both free and forced convection coefficients and the radiant heat factor to the environment, in addition to determining the power of the heat source. Heat transfer through conduction is ensured by the program. In the next part of the work, the adopted procedure of modelling the temperature field, the results of experimental tests and a summary will be presented.

2. THERMO-MECHANICAL MODEL OF MEASURING STAND

Bearing temperature has a significant influence on the motion resistance, therefore it is necessary to couple the heat source mechanical model (power loss in the bearing) with the FEM heat model [among others 4, 8]. A temperature increase is related to the reduction in kinematic viscosity of the lubricant base oil, which results in a reduction in viscous friction resistance and thus in a reduction in heat source power. Coupling the theoretical model of bearing power loss with FEM analysis requires an iterative approach. Such an approach is correct for the thermal steady-state, but inadequate for the transient state as the temperature changes with the operating time. Hence, the power lost in the bearing changes in some way as well, depending on the operating time. The approach presented in this paper concerns the thermal steady-state. Possible solution for transient analysis has been presented e.g. in paper [18].

2.1 Bearing power loss model

As already mentioned, the adoption of an appropriate power loss model is extremely important. According to the most recent models [2, 8] describing fast-running angular contact bearings, the total moment of motion resistance is the sum of the following components: moment resulting from the ball rolling friction ($M_{1(T)}$), reduced moment resulting from the spin phenomenon ($M_{s(red)}$) and viscous grease friction moment (M_v):

$$M = M_{1(T)} + M_{s(red)} + M_v \tag{1}$$

In this paper, the Musiał model [13] was adopted, which allows determining the moment of rolling friction of balls, which is described by the relation (2). The use of this relationship requires the determination of the contact forces Q_i and Q_o by analytical analysis or FEM simulation, which is a complex issue in itself and requires a considerable amount of calculation. Also, a value for the coefficient of rolling friction should be adopted.

$$M_{1(T)} = \left(\frac{d_m}{D} + 0.5\right) \sum_{j=0}^{j=Z-1} Q_j f_{kj} \tag{2}$$

Where:
d_m - bearing pitch diameter,
D - ball diameter,
Z - number of balls,
Q_j - j^{th} substitute contact force,
f_{kj} - j^{th} rolling friction coefficient.

The motion resistance moment resulting from the spin phenomenon can be described by relation (3) [10]. The power loss for the moment determined in this manner concerns the angular velocity of the spin, the calculation of which is quite complex, and dependencies describing this velocity can be found in the paper [3]. Knowing the angular velocity of the spin allows reduction the spin torque on the shaft. By knowing the contact parameters on a given raceway (force and size of the contact ellipse), the motion resistance moment from the spin phenomenon can be determined separately for the inner and outer raceway. The angular velocities of the spin strictly depend on the assumed hypothesis of gyroscopic moment distribution. The paper adopts the hypothesis of a controlled outer raceway, in which it is assumed that the ball rolls without sliding on this raceway. This hypothesis is very often accepted for bearing operation at a very high rotational speed and low external loads [3]. Due to the assumed hypothesis, the value of the spin moment on the outer raceway is zero and the whole spin moment is generated on the inner raceway.

$$M_s = \frac{3\pi\mu ZaQ}{8} \tag{3}$$

where:
μ - sliding friction coefficient,
Z - number of balls,
a - length of the longer semi-axis of the contact ellipse,
Q - contact force.

The motion resistance moment resulting from viscous friction is commonly determined based on the dependencies proposed by Palmgren [17]:

$$\begin{aligned} &M_v = 10^{-7} \cdot f_o \cdot (v_o \cdot n)^{2/3} \cdot d_m^3 \\ &\text{(for } v_o \cdot n \geq 2000\ cSt \cdot rpm) \\ &M_v = 160 \cdot 10^{-7} \cdot f_o \cdot d_m^3 \\ &\text{(for } v_o \cdot n < 2000\ cSt \cdot rpm) \end{aligned} \tag{4}$$

Where:
f_o - coefficient depending on the bearing type and lubrication method,
v_o - kinematic viscosity of the lubricant base oil (temperature dependent),
n - bearing velocity,
d_m - bearing pitch diameter.

Defining the magnitude of the contact forces is crucial in determining the values of the motion resistance moment from rolling friction (2) and spin phenomenon (3). To do this, the following are considered, Figure 1: contact forces Q_i and Q_o, centrifugal force F_c resulting

from the circulating movement of the ball around the bearing axis and gyroscopic moment M_g balanced by friction forces $\lambda_{i/oj}\frac{M_g}{D}$. The λ coefficient depends on the assumed hypothesis of the gyroscopic moment distribution. For the hypothesis of a controlled outer raceway λ_{ij}=0 and λ_{oj}=2. The equilibrium equations for vertical and horizontal direction are arranged. The angles of action of α_i and α_o contact forces and the forces themselves are unknown. Also, it is possible to make out the geometrical condition defining the mutual positions of the center of the ball and the centers of curvature of both raceways. An extended contact model [9] has been adopted for the described calculations, which in its assumptions considers the possibility of radial, elastic deformations of the rotating ring, which affect the values of forces and operating angles. It has been demonstrated that radial displacements resulting from high centrifugal forces increase the values of contact forces compared to the classical model [14]. A model of deformation has been adopted, which assumes that the balls limit the increase in the radial dimension of the ring [9, 15]. This radial displacement of the ring is implemented in the model in the geometric condition. For the case of rigid preload, a simplifying assumption is introduced, assuming that the angles of operation change by the same magnitude Δα from the initial value, with the angle α_i increasing and α_o decreasing [12]. This assumption allows for solving the described set of equations. The determined contact forces Q_i and Q_o are about 59 N for a nonrotating bearing. As the speed increases, the force on the outer raceway changes noticeably, reaching over 68 N at 10000 rpm.

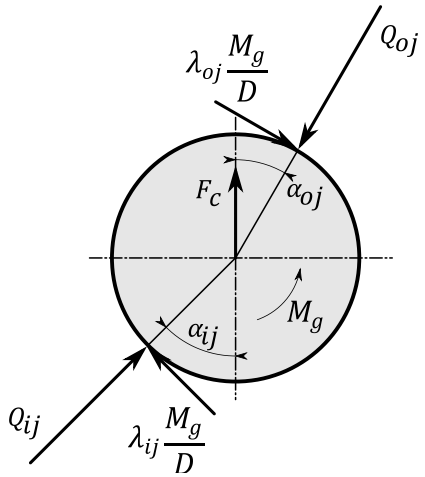

Fig. 1. Loading forces on the bearing ball

The contact forces, in themselves, are the subject of numerous research papers [among others 1, 16], but are also used to model spindle displacements [e.g. 7], or their dynamic properties [6].

2.2 Heat transfer model

As already mentioned, the modelling of the temperature field in FEM software requires that appropriate convection coefficients are assigned to all external surfaces. Figure 2 shows the design of a test rig where subsequent experimental research was conducted. The shaft is driven by an independent electrospindle supported by two high-speed angular contact bearings B7007-E-T-P4S in the "O" arrangement. Rigid preload is used, the value of which is measured indirectly by measuring the axial force using a piezoelectric insert. The value of the force was afterward converted into the value of relative mutual displacement of bearing rings, which corresponds to the preload.

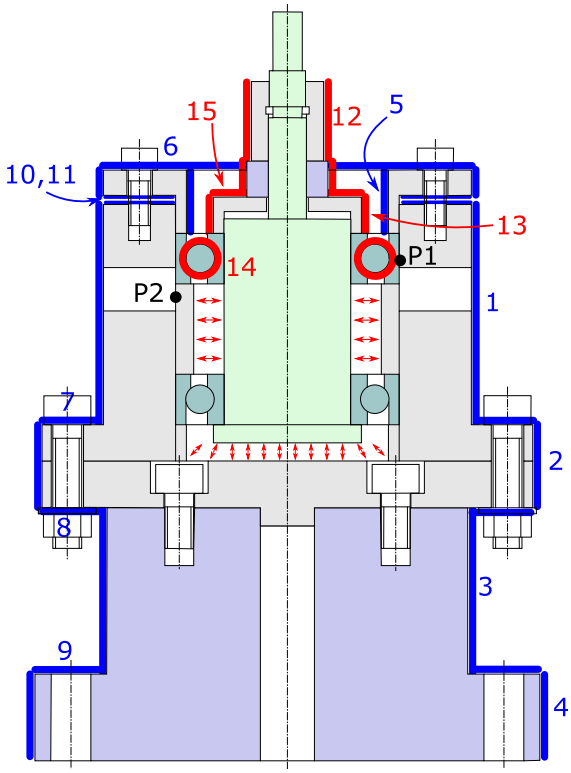

Fig. 2. Diagram of the test rig with specified surfaces to which convection in the simulation is assigned

The blue colour was used to determine the surfaces to which free convection was assigned, while the red colour was used for forced convection. The available literature describes dependencies on the determination of the Nusselt number depending on the location of the surface or its shape (flat, cylindrical surface). The Nusselt number is the number of similarity from which it is possible to determine the convection coefficient according to the relation (5). The fluid heat conduction coefficient λ_p is not the same as the coefficients associated with gyroscopic moment distribution.

$$Nu = \frac{\alpha l}{\lambda_p} \tag{5}$$

Where:

α - heat transfer coefficient (convection) in $\left[\frac{W}{m^2 \cdot K}\right]$,

l - characteristic dimension,

λ_p - heat conduction coefficient of the liquid in $\left[\frac{W}{m \cdot K}\right]$.

Table 1. Dependencies applied for the determination of Nusselt numbers

No.	Nusselt number	Surfaces	Source
1	$Nu_L = \left[\frac{Pr}{2.435 + 4.884 \cdot Pr^{0.5} + 4.953 \cdot Pr}\right]^{0.25} \cdot (Ra_L)^{0.25}$	1, 2, 3, 4, 5	[11]
2	$Nu_L = 0.27 \cdot (Ra_L)^{0.25}$	6, 7, 9, 10	[11]
3	$Nu_L = 0.54 \cdot (Ra_L)^{0.25}$	8, 11	[11]
4	$Nu = 0.11 \cdot [Pr \cdot 0.5 \cdot Re^2 + Gr]^{0.35}$	12, 13	[2]
5	$Nu = 0.33 \cdot Re^{0.5}$	15	[2]
6	$Nu = 0.33 \cdot Re_D^{0.5} \cdot Pr^{0.4}$	14	[3]

Table 1 shows all the relationships applied to determine Nusselt numbers. The calculation of Nusselt numbers often requires the enumeration of other similarity numbers such as Rayleigh (Ra), Reynolds (Re) or Grashof (Gr), the relevant relationships can be found in the available literature [e.g. 11]. The Reynolds number for a rotating ball (Re_D) can be calculated from the relationship given by Harris [3]:

$$Re_D = \frac{\omega D^2}{v} \tag{6}$$

The value of the free convection coefficient depends to a large extent on the temperature difference between a given surface and the surrounding area, which results from the Rayleigh number (Ra_L). As the surface temperature increases, an increasing amount of heat is released into the environment. Figure 3 shows sample values of free convection coefficients depending on the surface temperature, assuming the ambient temperature of 20°C. The value of the coefficient varies within a few $\frac{W}{m^2K}$. Based on Table 1 and dependence (5), values of free convection coefficients were calculated for all surfaces of the test rig.

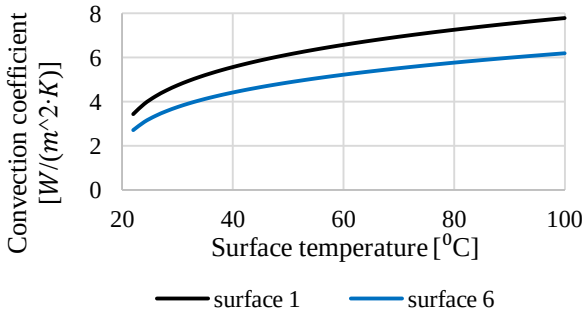

Fig. 3. Free convection coefficient of the sample surfaces as a function of their temperature

Based on the calculations carried out, it can be concluded that the value of the forced convection coefficient does not depend to a large extent on the difference in surface and ambient temperature. For high speeds, the value of this coefficient is practically the same regardless of the temperature difference, however it has been determined as for free convection. The forced convection coefficient is greatly influenced by the linear relative velocity of the surface relative to the stationary environment. Figure 4 shows the results of calculations of the effect of bearing rotational speed on the magnitude of forced convection coefficients of sample surfaces (at their temperature of 40°C). Forced convection is characterized by a much higher amount of heat transferred to the environment concerning free convection. For the tested rotational speeds, the convection coefficient reached even more than 200 $\frac{W}{m^2K}$ at maximum speeds.

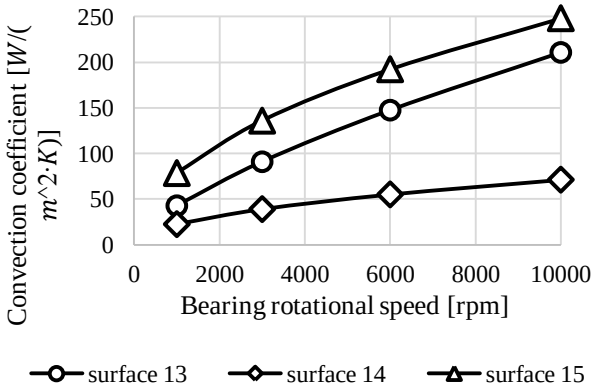

Fig. 4. Influence of rotational speed on the value of forced convection coefficient of selected surfaces

2.3 Numerical model of a test rig

To model the temperature field, a CAD model of the test rig was developed. Simulations of heat distribution and temperature field were performed in Ansys v. 13. Figure 5 shows a test rig model with a superimposed finite element mesh, and Figure 6 shows examples of steady-state temperature simulation results. As shown in Figure 2, appropriate convection coefficients are assigned to the surfaces as a function of their temperature. Theoretical models (1), (2), (3) and (4) were applied to determine the amount of heat

generated in bearings, in which the values of rolling and sliding friction coefficients were chosen arbitrarily in the first place. The heat source was divided into both raceways - a part of power corresponding to rolling friction and the spin phenomenon was divided based on analytical relations, while the part of power corresponding to viscous friction was divided equally to both raceways. Results of the initial simulations were characterized by significant temperature values, significantly exceeding the values obtained during the experimental research. So, it was decided to attach to the rig model a steel plate constituting the base (as in the case of the experimental stand) with a relatively large area and large thermal capacity. Appropriate values of free convection coefficient have been assigned to the surfaces of the plate.

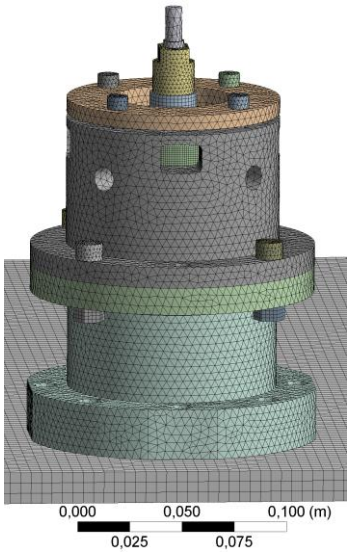

Fig. 5. CAD model of test rig with superimposed finite element mesh

The value of the bearing's motion resistance and thus the power loss depends on the kinematic viscosity of the lubricant base oil, which depends on temperature. Therefore, after the simulation, the temperature was read from several points - the balls and rings of the bearing, which was averaged and the power lost in the bearing (heat source) was recalculated. The procedure was repeated until the power of the heat source and the temperature values at the rig were slightly changing. The limit value was assumed to be a temperature change of less than 0.01°C. The number of steps of such an iterative approach depended on the value of the tested rotational speed - the higher the more steps were necessary. For the maximum tested rotational speed of 10000 rpm it was 7 steps, and for the minimum 500 rpm 3 steps. Figure 7 shows the changes in heat source power in individual iteration steps for several speeds. Due to the temperature increase, the kinematic viscosity of the lubricant base oil decreases, as well as the power lost due to the viscosity resistance. Therefore, in the second iteration step, the power of the heat source can be much lower. Depending on the speed, the power drop ranges from 2.4% (500 rpm) to 46.1% (10000 rpm). After the last step, for a given speed, temperature were read out from the points of interest of the rig in which temperature was measured in the experimental studies.

a)

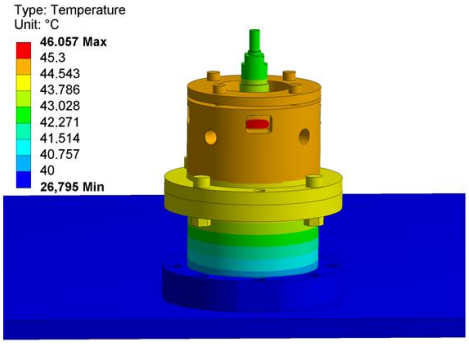

b)

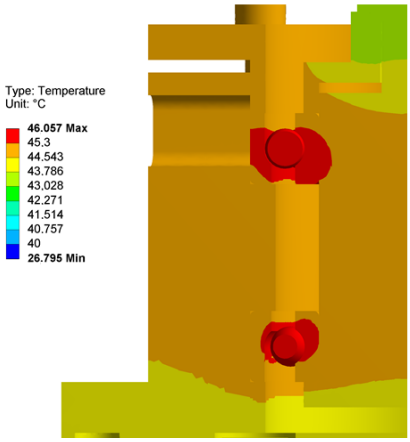

Fig. 6. Examples of simulation results (n=6000 rpm, δa=8.4 μm)

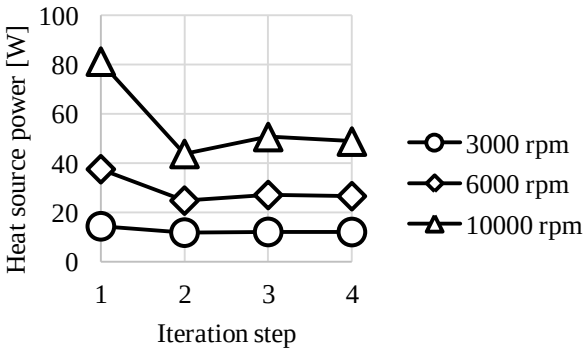

Fig. 7. Changes in heat source power

According to the presented methodology, simulation tests were carried out to simulate the effect of speed on the temperature in steady-state. The preload value of δ_a=8.4 μm, used in later experiments, was assumed in the tests. The simulations did not take into account the motion of the balls around the axis of rotation of the bearing, which is a certain simplification, but the temperature distribution should reflect the reality as the heat source was assigned to the whole length of both

raceways. Regardless of the speed, the differences between the temperature of the balls and, for example, the external surface of the body are relatively small. For example, for speeds of 6000 rpm, they do not exceed 2°C. Figure 8 shows the obtained temperature on the outer ring (point P1 in Figure 2) and the spacer between bearings (point P2 in Figure 2). The temperature values in both places are very similar, and the results obtained are practically linear concerning speed. The temperature at these points was measured in the experimental research, as described below.

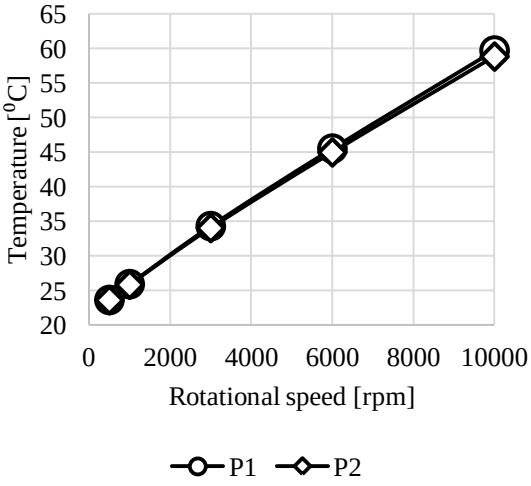

Fig. 8. Influence of speed on the temperature at points P1 and P2

3. EXPERIMENTAL RESEARCH

To verify the simulations, experimental research was carried out to determine the effect of rotational speed on test rig temperature. As already mentioned, the bearings preload is rigid and it was measured by checking the value of axial force with the piezoelectric sensor. Afterward, the value of this force was converted based on the theoretical contact models into the relative displacement of bearing rings, which corresponds to the preload value. The preload was set to 360 N, which corresponds to a displacement of about 8.4 µm.
Temperature were measured with Dallas 18B20 contact sensor, the measurement accuracy of which guaranteed by the manufacturer is +/- 0.5°C, Optris CTIlaser LTF pyrometer with a measurement accuracy of +/- 1.5%, and the VIGOcam v50 thermo vision camera. Contact sensors were used to measure the temperature of the outer ring of one of the bearings (point P1) and the spacer between the bearings (point P2). A laser pyrometer was used to measure temperature of the ball's contact zone with the raceway. This was possible thanks to application of open bearings and accessing to one of the bearings from the top of test rig. Figure 9 shows a view of the test rig where we can see the contact sensor wires and the pyrometer laser light dot. The surfaces measured with a thermovision camera were coated with matte paint with a coefficient of emission of 0.81 [5], which was applied to process the obtained results in the camera manufacturer's software.

Fig. 9. View of the test rig

Figure 10 shows the obtained courses of the measured temperature values in point P1 (bearing outer ring) and P2 (spacer sleeve) for the tested rotational speeds. Depending on the speed, the temperature stabilizes at a certain value at different times. In any case, the temperature on the spacer is lower than on the bearing outer ring. For model tests, only temperature for the steady-state thermal condition of the rig are relevant.

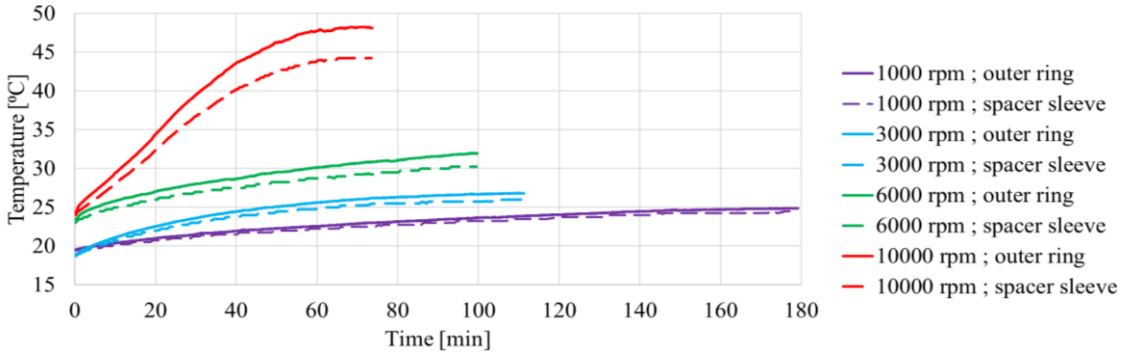

Fig. 10. The temperature change of the outer ring and spacer sleeve for the test speeds

Figure 11 shows images from thermo vision camera in a steady-state for all speeds considered. The infrared thermo vision camera was used to compare the actual temperature field with FEM results and to be able to read the temperature from any point on the rig.

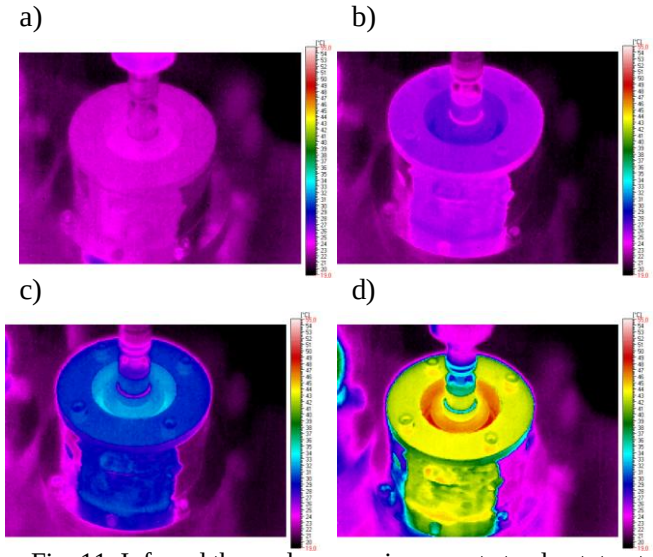

Fig. 11. Infrared thermal camera images at steady-state at a) 1000 rpm, b) 3000 rpm, c) 6000 rpm, d) 10000 rpm

Figure 12 shows the results of experimental tests, i.e. temperature for a steady-state thermal condition. The temperature of the bearing outer ring, spacer sleeve, contact point and housing (in the middle of its height) are included. As it could be presumed, temperature increase with speed. For 1000 rpm they range from 22.6°C on the body to 27.9°C at the point of contact and for maximum considered speed from 41.5°C to 60.2°C.

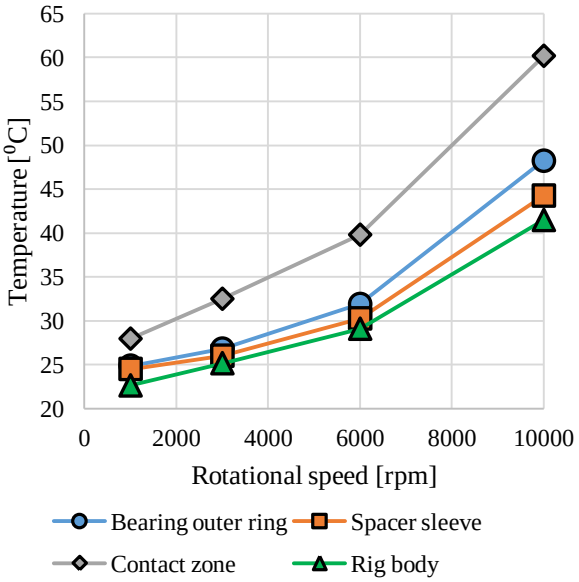

Fig. 12. Influence of the speed on the temperature for the thermally determined rig

A comparison of temperature values of bearing ring obtained by experiment and simulation is shown in Figure 13. Originally obtained values in the FEM environment for the rolling friction coefficient and sliding friction coefficient of the spin selected arbitrarily proved to be too high (too high power of the heat source). Therefore, it was decided to adjust their values based on experimental measurements of the bearing's motion resistance moment so that the determined motion resistance moment (model) is close to the one measured experimentally. The finally applied values of the coefficients were: f_{kj}=0.0002 and μ=0.01.

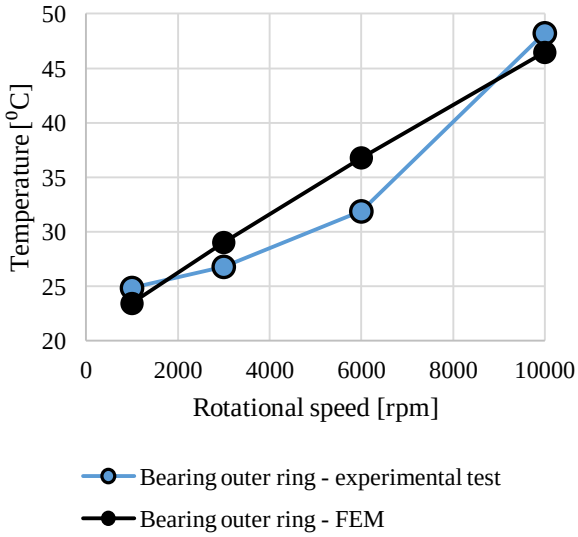

Fig. 13. Influence of the speed on the temperature for the steady-state thermal condition thermally of test rig - summary of test and simulation results

4. CONCLUSIONS

The paper presented results of thermal analysis of a test rig for testing angular contact ball bearings. The purpose of this analysis was to determine the temperature distribution for different bearing rotational speeds at specific preload. The knowledge of this temperature enables the assessment of thermal deformations in the bearing, which influence the contact forces and thus the motion resistance of bearing. The research was carried out using the finite element method and the results obtained were compared with the results of experimental research. The comparative assessment allows for high compliance in terms of quality, i.e. increasing temperature with increasing speed. The quantitative evaluation, on the other hand, indicates the need to improve the numerical model, which will be further investigated.

5. REFERENCES

1. Antoine, J-F., Abba, G., Molinari, A., (2006). *A new proposal for explicit angle calculation in angular contact ball bearing*, Journal of Mechanical Design, **128**(2), 468-478

2. Buchman, K., Jungnickel G., (1978). *Heat transfer in manufacturing devices* (in polish), pp. 280,

Publishing House of Wroclaw University of Technology, Wrocław.
3. Harris, T. A., Kotzalas M. N., (2007). *Rolling bearing technology, 5th edition: advanced concepts of bearing technology,* pp. 352, CRC Press, Boca Raton
4. Holkup, T., Cao, H., Kolar, P., Altintas, Y., Zeleny, J., (2010). *Thermo-mechanical model of spindles,* CIRP Annals – Manufacturing Technology, **59**, 365-368.
5. Honnerova, P., Martan, J., Vesely, Z., Honner, M., (2017). *Method of emissivity measurement of semitransparent coatings at ambient temperaturę,* Scientific Reports **7**(1), pp. 7: 1386.
6. Chen, J-S., Hwang, Y-W., (2006). *Centrifugal force induced dynamics of a motorized high-speed spindle,* The International Journal of Advanced Manufacturing Technology, **30** (1), 10-19.
7. Jędrzejewski, J., Kwaśny, W., (2010). *Modelling of angular contact ball bearings and axial displacements for high-speed spindles,* CIRP Annals – Manufacturing Technology, **59**, 377-382.
8. Jin, C., Wu B., Hu, Y., (2012). *Heat generation modeling of ball bearing based on internal load distribution,* Tribology International, **45**, pp. 8-15.
9. Kosmol, J., (2019). *An extended contact model of the angular bearing,* Journal of Theoretical and Applied Mechanics, **59**(1), 59-72.
10. Kosmol, J., (2016). *Determination of motion resistances in high-speed spindle angular bearings*, pp. 93, Publishing House of Silesian University of Technology, Gliwice.
11. Latif, M. J., (2009). *Heat Convection, second edition*, pp. 543, Springer-Verlag Berlin Heideberg.
12. Liao, N. T., Lin, J. F., (2002). *Ball bearing skidding under radial and axial loads,* Mechanism and Machine Theory, **37**, pp. 91-113.
13. Musiał, J., Styp-Rekowski, M., (1999). *Analytically-experimental method of determining the rolling friction coefficient* (in polish). Proceedings of „Problems of unconventional bearing configuration", pp. 59-65, Polish Tribology Society, Łódź.
14. Muszyński, M., (2019). *Simulation tests of the influence of elastic radial deformations of the rotating ring on the contact forces in angular bearing* (in polish), Modelling in Engineering, **40**(71), pp. 63-68.
15. Muszyński, M., (2018). *Radial deformations in high-speed bearing rings due to centrifugal forces (in polish),* Modelling in Engineering, **37**(68), pp. 85-90.
16. Noel, D., Ritou, M., Furet, B., Le Loch, S., (2013). *Complete analytical expression of the stiffness matrix of angular contact ball bearings,* Journal of Tribology, **135**, pp. 041101-1:041101-8.
17. Palmgren, A., (1959). *Ball and roller bearing engineering, 3rd edition*, pp. 264, SKF industries, Philadelphia.
18. Wang, H., Cai, Y., Wang, H., (2017). *A dynamic thermal-mechanical model of the spindle-bearing system,* Mechanical Sciences, **8**, pp. 277-288.
19. Šooš, Ľ. (2012). *Radial ball bearings with angular contact in machine tools,* Performance of bearings, edited by Rakesh Sehgal, pp. 49-92, IntechOpen, Rijeka.

Received: September 08, 2020 / Accepted: December 15, 2020 / Paper available online: December 20, 2020